The rotational excitation temperature of the λ6614 DIB carrier.

J. Cami[1], F. Salama[1], J. Jiménez-Vicente[2], G. Galazutdinov[3,4] and J. Krelowski[5]

jcami@mail.arc.nasa.gov

ABSTRACT

Analysis of high spectral resolution observations of the λ6614 DIB line profile show systematic variations in the positions of the peaks in the substructure of the profile. These variations can only be understood in the framework of rotational contours of large molecules, where the variations are caused by changes in the rotational excitation temperature. We show that the rotational excitation temperature for the DIB carrier is of the order 10-40 K – much lower than the gas kinetic temperature – indicating that for this particular DIB carrier angular momentum buildup is not very efficient. The rotational constant indicates that the carrier of this DIB is smaller than previously assumed : 7–22 C atoms, depending on the geometry.

The rotational excitation temperature of the λ6614 DIB carrier.

J. Cami[1], F. Salama[1], J. Jiménez-Vicente[2], G. Galazutdinov[3,4] and J. Krelowski[5]

jcami@mail.arc.nasa.gov

ABSTRACT

Analysis of high spectral resolution observations of the λ6614 DIB line profile show systematic variations in the positions of the peaks in the substructure of the profile. These variations can only be understood in the framework of rotational contours of large molecules, where the variations are caused by changes in the rotational excitation temperature. We show that the rotational excitation temperature for the DIB carrier is of the order 10-40 K – much lower than the gas kinetic temperature – indicating that for this particular DIB carrier angular momentum buildup is not very efficient. The rotational constant indicates that the carrier of this DIB is smaller than previously assumed : 7–22 C atoms, depending on the geometry.

Subject headings: ISM: lines and bands, ISM: molecules

1. Introduction

The Diffuse Interstellar Bands (DIBs) are over 300 interstellar absorption bands commonly observed toward reddened stars from the UV to the near-IR, and whose carrier molecules are still unidentified (Herbig 1995; Snow 2001; Krelowski 2003). The identification of the carriers of these bands remains an important problem in astronomy to date and the current consensus on the nature of the carriers is that they are probably large

[1]NASA Ames Research Center, MS 245-6, Moffett Field, CA 94035, USA

[2]Depto. Física Teórica y del Cosmos,Fac. de Ciencias. Univ. de Granada,Av. Fuentenueva s/n, 18071 Granada, Spain

[3]Korean Astronomy Observatory, Optical Astronomy Divison, 61-1, Whaam-Dong, Yuseong-Gu, Daejon 305-348, Korea

[4]Special Astrophysical Observatory, Nizhnij Arkhyz 357147, Russia

[5]Center for Astronomy, Nicolaus Copernicus University, Gagarina 11, 87-100 Torún, Poland

carbon-bearing molecules which reside ubiquitously in the interstellar gas (Ehrenfreund & Charnley 2000). The most promising carrier candidates are carbon chains, Polycyclic Aromatic Hydrocarbons (PAHs), and fullerenes (Salama et al. 1996, 1999; Foing & Ehrenfreund 1994, 1997; Ehrenfreund & Foing 1996; Schulz et al. 2000; Motylewski et al. 2000). Studies on the environmental behavior of DIB carriers suggest that the strength of the DIBs results from an interplay between ionization, recombination, dehydrogenation and destruction of chemically stable, carbonaceous species (Herbig 1995; Cami et al. 1997; Sonnentrucker et al. 1997; Vuong & Foing 2000). The molecular nature of the DIB carriers is supported by the detection of substructures in the line profiles of some DIBs (Sarre et al. 1995; Ehrenfreund & Foing 1996; Krelowski & Schmidt 1997; Le Coupanec et al. 1999; Walker et al. 2001; Galazutdinov et al. 2002). Furthermore, a recent analysis of the profile of the strongest DIB (λ4428) shows a Lorentzian profile remarkably consistent with rapid internal conversion in a molecular carrier (Snow et al. 2002).

In this paper, we present an analysis of high-resolution observations of the λ6614 DIB in so-called "single-cloud" lines of sight. The profiles show a systematic variation in the wavelengths of the observed substructure peaks. We show that these variations can only be explained in terms of changes in the rotational excitation temperature in rotational contours of a large molecule. The particular band profile of this DIB also allows one to calculate the rotational excitation temperature.

2. The λ6614 DIB profile

The λ6614 DIB was first observed at high resolution by Sarre et al. (1995), revealing a clear triple-peak substructure and a red degraded wing (see Fig. 1). In a few stars, a weaker fourth and a fifth peak show up at longer wavelengths. As these are only clearly observed in two of our spectra, we will not discuss these peaks in this paper. The substructures are intrinsic to the band profile, as the same profile shape is observed in lines-of-sight that only cross one interstellar cloud.

The very presence of these substructures have been explained by two different scenarios. The most popular explanation is that the profile is due to unresolved rotational contours of a large molecule, in which the three peaks represent individual branches of a ro-vibronic transition. Rotational contour calculations have been performed by Cossart-Magos & Leach (1990) for PAHs, Edwards & Leach (1993) for fullerenes and by Schulz et al. (2000) for linear chains. Ehrenfreund & Foing (1996) analyzed the profiles of the λ6614 DIB and compared them to calculated rotational contours, concluding that the carrier of the λ6614 DIB has a rotational constant compatible with PAHs larger than 40 C-atoms, chains of 12-18 C-atoms,

30 C-atom rings or C_{60} fullerene compounds.

Alternatively, the substructures might be due to isotope shifts in large, highly symmetric molecules (Webster 1996). In this scenario, the individual peaks correspond to entities of the same molecule with a different number of ^{13}C atoms. The relative intensities of the peaks then determine the abundances of the isotopic varieties (see e.g. Walker et al. 2000).

3. The λ6614 DIB profile variations

Recently, Galazutdinov et al. (2002) presented new high-resolution ($R \approx 220000$), high S/N observations of the λ6614 DIB toward single-cloud lines-of-sight, clearly showing variability in the precise wavelengths of the peaks, and in the intensity ratios. In this paper, we analyze those same observations; we therefore refer to Galazutdinov et al. (2002) for more details concerning the observational details.

The profiles of the interstellar Na I or K I lines toward our target stars are narrow, and generally show only one main component (Galazutdinov et al. 2002), confirmed also by ultra-high resolution observations for various interstellar lines which are now available (e.g. Welty et al. 1994; Welty & Hobbs 2001). The observed DIB profiles are therefore intrinsic.

Fig. 1 shows the profiles of the λ6614 DIB centered on the central peak. It is clear that there are considerable variations in the exact positions of the remaining two main peaks with respect to this central peak. The redward peak (Peak 3) shows clear variations in wavelength relative to the central peak which are much larger than the individual variations in radial velocity, and therefore these variations are intrinsic. To better assess these variations, we proceeded in the following way. In all proposed explanations for the substructure of the λ6614 DIB, the observed profile is composed of individual bands. In the rotational contour framework, these bands correspond to unresolved ro-vibronic branches; in the isotope shift scenario they correspond to different isotopomers. To accurately determine the peak positions of these individual components, we need to decompose the profile into its components, rather than measuring the peak positions directly in the full profile.

Galazutdinov et al. (2002) showed that nearly perfect fits to the observed line profiles can be achieved by fitting about 5 Gaussians to the line profiles. The three main Gaussian components correspond to the three main peaks observed in the line profile; a fourth and fifth component are required for the additional peaks and/or the red wing. We followed a similar approach to decompose the profile into Gaussian components. The fitting routine provides a formal error on the derived parameters (such as peak position), but this error estimate is generally quite optimistic, as it does not deal with systematic errors (such as the components

not being Gaussians). We therefore followed a statistical approach in which we determined the noise level on the spectra from the parts outside the λ6614 DIB, subsequently added random noise with the same rms to the data, and then fitting the profile. This procedure was repeated 100 times for each spectrum, and subsequently each parameter value was taken to be the average of these 100 simulations, with the standard deviation providing a more realistic error estimate on these parameters. Using the wavelengths of the central peak (Peak 2 in Fig. 1), we then shifted the individual profiles in velocity space to the same "rest" wavelength of 6613.56 Å for the central peak (Galazutdinov et al. 2000).

Fig. 2 shows the peak positions for each of the three main peaks as a function of the peak separation between the first and the third peak. The variations in the wavelengths of the sub-peaks now become much more obvious. When the redward peak (Peak 3) shifts to longer wavelengths relative to the central peak, the blueward peak (Peak 1) *systematically* shifts to shorter wavelengths. Whereas Peak 1 shifts by about 0.03 Å(one resolution element), Peak 3 shifts by double that amount.

These variations rule out the scenario in which the substructures are due to isotope shifts : in such a case, the wavelengths of the individual peaks should be the same for each line-of-sight. On the other hand, the observed variations are completely consistent with the substructure being due to unresolved rotational contours, and the observed variations due to changes in only one parameter : the rotational excitation temperature.

4. Rotational contours

In the framework of rotational contours, the three peaks in the λ6614 DIB correspond to unresolved PQR-type branches of some molecular species. Although exact profile shapes for different molecules need to be calculated on an individual basis, properties of the carrier molecules can be inferred from a more general approach that we follow here.

For the case of a spherical top or a linear molecule (other geometries are discussed in Sect. 6), the energies of the rotational levels within a vibronic band are determined by the rotational constant B and the rotational quantum number J. For a given rotational level J, the frequencies of the P and R transitions relative to the corresponding Q transition can then be written as

$$\Delta\nu_{RQ} \equiv \nu_R - \nu_Q = 2(J+1)(B'' + \Delta B) \quad (1)$$

$$\Delta\nu_{QP} \equiv \nu_Q - \nu_P = 2J(B'' + \Delta B) \quad (2)$$

where the double primes refer to the lower vibronic level and ΔB is the difference in rotational constants between the upper and lower vibronic level. All other things being equal, the peak

absorption will arise from the most populated rotational level in the lower vibronic state. Assuming an LTE-like population distribution of the rotational levels in this lower state, it is straightforward to show that the most populated rotational level is (see e.g. Bernath 1995, p.173)

$$J_{\max} = \sqrt{\frac{kT_{\rm rot}}{2hcB''}} - \frac{1}{2} \tag{3}$$

with B'' in cm^{-1}. Eqs. (1), (2) and (3) nicely show how the peaks of the R and P branches move away from the Q branch peak (at a different rate) when $T_{\rm rot}$ increases : as $T_{\rm rot}$ increases, $J_{\max}$ becomes larger, and therefore both peak separations increase. This corresponds exactly to what we observe (see Fig. 2), and therefore the central peak (Peak 2) in the λ6614 DIB must correspond to the unresolved Q-branch, and Peak 1 and 3 the R and P branch respectively.

Dividing Eq. (2) by Eq. (1), solving for J and substituting J by Eq. (3) yields

$$\frac{T_{\rm rot}}{B''} = \frac{hc}{2k}\frac{(1+f)^2}{(1-f)^2} \tag{4}$$

where $f = \Delta\nu_{QP}/\Delta\nu_{RQ}$. Similarly, by adding Eqs. (1) and (2) one can find that

$$T_{\rm rot} \cdot B'' = \frac{hc(\Delta\nu_{RP})^2}{8k\left(1+\frac{\Delta B}{B''}\right)^2} \tag{5}$$

where $\Delta\nu_{RP} = \nu_R - \nu_P$. Multiplying Eqs. (4) and (5) then yields

$$T_{\rm rot} = \frac{hc}{4k}\frac{(\Delta\nu_{RP})}{(1+\frac{\Delta B}{B''})}\frac{1+f}{1-f} \approx \frac{hc}{4k}(\Delta\nu_{RP})\frac{1+f}{1-f} \tag{6}$$

Finally, by subtracting Eq. (2) from Eq. (1), the rotational constant can be estimated :

$$B'' \approx B'' + \Delta B = (\Delta\nu_{RQ} - \Delta\nu_{QP})/2 \tag{7}$$

In both Eqs. (6) and (7) the common approximation has been used that $\Delta B/B''$ is generally negligible (at most a few percent) for large molecules.

5. Results

Table 1 lists the measured peak separations (in cm^{-1}) for the three main peaks of the λ6614 DIB profile and the excitation temperature and rotational constant derived using

Eqs. (6) and (7). As the uncertainties on $T_{\rm rot}$ and B'' are asymmetric, we also listed minimum and maximum values allowed within the uncertainties. The peak separation between Peak 1 and 3 is in good agreement with the values published by Ehrenfreund & Foing (1996).

As the carrier molecule for the λ6614 DIB should be the same for all lines-of-sight considered, the derived rotational constant should also be the same. Table 1 shows that the individually derived rotational constant differ by about a factor of 4 with a weighted mean value of $B'' = 19.0\ 10^{-3}$ cm^{-1}.

Also the uncertainties on the derived rotational excitation temperature can be large. Eq. (6) shows that for f close to unity, small errors on f have a large impact on the resulting temperature; this is reflected into the minimum and maximum possible excitation temperatures listed in Table 1. It should be noted that the rotational excitation temperature therefore is best determined for those sources which have the lowest excitation temperature. Note also that if we use the weighted mean value for the rotational constant instead of the individually derived rotational constants for each line-of-sight (i.e. replace the values for B'' in Table 1 by $19.0\ 10^{-3}$ cm^{-1}), the derived excitation temperatures would be in the range 16-23 K.

The derived rotational excitation temperature is clearly significantly lower than the kinetic gas temperature in the same lines-of-sight (see values in Table 1 taken from Savage et al. 1977). Only for two sources is the gas temperature within the uncertainties of the rotational excitation temperatures.

6. Discussion

The observed variations in the peak positions of the substructures in the λ6614 DIB can be explained both qualitatively and quantitatively by using the rotational contour formalism, and varying only the rotational excitation temperature.

It is surprising though that the derived rotational excitation temperature is much lower than the kinetic gas temperature, as it has been argued that the rotational excitation temperature should actually be higher than the gas temperature (Rouan et al. 1992, 1997; Le Coupanec et al. 1999; Mulas 1998; Malloci et al. 2003). One might argue that the assumption of LTE in the rotational population distribution would lead us to significantly underestimate the "true" rotational excitation temperature. However, Monte Carlo simulations that follow the detailed balance in the rotational populations and yield a statistical equilibrium taking into account radiative processes show that the population distribution over J is very similar to a thermal distribution (Mulas 1998). Therefore, the LTE assumption cannot be the cause

for such differences in the resulting excitation temperature. Moreover, these papers predict typical values for J_{max} of $\sim$100. From Eqs. (1) and (2), one can easily calculate the ratio $J_{max}/(J_{max}+1)$, and it is clear that this ratio is significantly lower than unity for at least three lines-of-sight, indicating that J_{max} must be much lower than predicted on theoretical grounds. Clearly, either the rotational excitation processes (rocket effect, IVRET, ...) included in those calculations are less important than assumed, or the relaxation processes are more efficient. It should however be emphasized that these calculations are generally carried out for large ($\sim$ 100 C atoms) PAH-like molecules. Smaller molecules or molecules of a different geometry might show a different excitation and relaxation balance. The rotational constants we derive here are indeed indicative of smaller molecules. Adopting a similar approach as Ehrenfreund & Foing (1996) to estimate the size of the λ6614 DIB carrier, we find PAHs of 18-22 C atoms, or linear C chains of about 7-10 C atoms.

The question then remains how general the adopted formalism is for the interpretation of rotational contours. In a more general case, the rotational energies and allowed transitions will also depend on the remaining rotational constants A and C, and each J level is split up into $2J+1$ levels with an additional energy term $(A-B)K^2$ for a prolate symmetric top or $-(A-C)K^2$ for an oblate rotor with $K=-J,\ldots,+J$. For parallel transitions ($\Delta K=0$), there are then $2J+1$ stacks of P, Q and R branches. For transitions with the same J but different K, the frequencies of these transitions will change by $(\Delta A-\Delta B)$ or $-(\Delta A-\Delta C)$; these shifts are generally small, and the overall shape of the profile in terms of peak positions will not change much. For perpendicular bands ($\Delta K=\pm 1$), the transitions now shift by $\pm(A-B)K$ or $\pm(A-C)K$. For each K, there are now two sets of P, Q and R branches. One set is shifted to the blue, the other to the red. All branches become broader, and the P and R branches will either move away from the Q branch (oblate tops) or move closer to the Q branch (prolate tops) by an amount which is now determined by the rotational constants A and C. For the case of perpendicular bands, we therefore either overestimate the rotational excitation temperature for an oblate case, or underestimate it for a prolate case.

For these more complex geometries, detailed calculations are required to accurately determine the molecular and physical parameters. Such calculations are currently in progress and will be presented in a future paper.

7. Conclusions

We have analyzed high-resolution and high signal to noise spectra of the λ6614 DIB toward single-cloud lines of sight. The spectra clearly show a systematic shift in the relative

peak position of two of the subpeaks. We show that such an effect cannot be understood if the substructure is due to isotope shifts. On the other hand, a simple analysis shows that this effect can be explained both qualitatively and quantititatively by rotational contours in which only the rotational excitation temperature changes. The derived rotational constants are larger than previously derived, and the λ6614 DIB carrier must therefore be a smaller molecule (7–22 C atoms depending on the geometry). The rotational excitation temperatures are low, indicating that for this particular DIB carrier, rotational excitation is not very efficient.

We would like to thank Bernard Foind and Xander Tielens for stimulating discussions. JC gratefully acknowledges the support of the National Research Council's Research Associateship Program. This work is supported by the NASA APRA Program (RTOP N^o 188-01-03-01). JK is grateful to the Polish State Committee for Scientific Research for the support under the grant 2 P03D 019 23

REFERENCES

Bernath P.F., 1995, Spectra of Atoms and Molecules. Oxford University Press, Inc., New York

Cami J., Sonnentrucker P., Ehrenfreund P., Foing B.H., 1997, *A&A* 326, 822

Cossart-Magos C., Leach S., 1990, *A&A* 233, 559

Edwards S.A., Leach S., 1993, *A&A* 272, 533

Ehrenfreund P., Charnley S.B., 2000, *ARA&A* 38, 427

Ehrenfreund P., Foing B.H., 1996, *A&A* 307, L25

Foing B.H., Ehrenfreund P., 1994, *Nat* 369, 296+

Foing B.H., Ehrenfreund P., 1997, *A&A* 317, L59

Galazutdinov G., Moutou C., Musaev F., Krełowski J., 2002, *A&A* 384, 215

Galazutdinov G.A., Musaev F.A., Krełowski J., Walker G.A.H., 2000, *PASP* 112, 648

Herbig G.H., 1995, *ARA&A* 33, 19

Krelowski J., 2003, In: *Solid State Astrochemistry*, pp. 147–+

Krelowski J., Schmidt M., 1997, *ApJ* 477, 209+

Le Coupanec P., Rouan D., Moutou C., Léger A., 1999, *A&A* 347, 669

Malloci G., Mulas G., Benvenuti P., 2003, *A&A* 410, 623

Motylewski T., Linnartz H., Vaizert O., et al., 2000, *ApJ* 531, 312

Mulas G., 1998, *A&A* 338, 243

Rouan D., Leger A., Le Coupanec P., 1997, *A&A* 324, 661

Rouan D., Leger A., Omont A., Giard M., 1992, *A&A* 253, 498

Salama F., Bakes E.L.O., Allamandola L.J., Tielens A.G.G.M., 1996, *ApJ* 458, 621+

Salama F., Galazutdinov G.A., Krełowski J., Allamandola L.J., Musaev F.A., 1999, *ApJ* 526, 265

Sarre P.J., Miles J.R., Kerr T.H., et al., 1995, *MNRAS* 277, L41

Savage B.D., Drake J.F., Budich W., Bohlin R.C., 1977, *ApJ* 216, 291

Schulz S.A., King J.E., Glinski R.J., 2000, *MNRAS* 312, 769

Snow T.P., 2001, *Spectrochimica Acta* 57, 615

Snow T.P., Zukowski D., Massey P., 2002, *ApJ* 578, 877

Sonnentrucker P., Cami J., Ehrenfreund P., Foing B.H., 1997, *A&A* 327, 1215

Vuong M.H., Foing B.H., 2000, *A&A* 363, L5

Walker G.A.H., Bohlender D.A., Krełowski J., 2000, *ApJ* 530, 362

Walker G.A.H., Webster A.S., Bohlender D.A., Krełowski J., 2001, *ApJ* 561, 272

Webster A., 1996, *MNRAS* 282, 1372

Welty D.E., Hobbs L.M., 2001, *ApJS* 133, 345

Welty D.E., Hobbs L.M., Kulkarni V.P., 1994, *ApJ* 436, 152

This preprint was prepared with the AAS LaTeX macros v5.2.

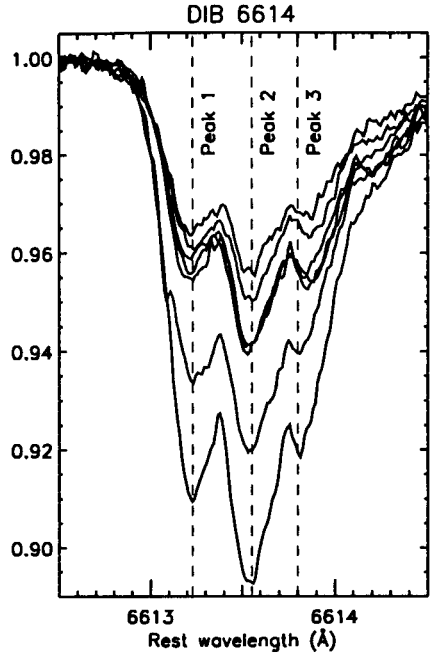

Fig. 1.— The profiles of the λ6614 DIB for the observed stars. All profiles are centered on the central peak (Peak 2). Note how the position of the redward peak (Peak 3) clearly changes from one line of sight to another. At the same time, the width of the sub-peaks seems to become marginally larger. For an identification of the individual spectra, see Galazutdinov et al. (2002)

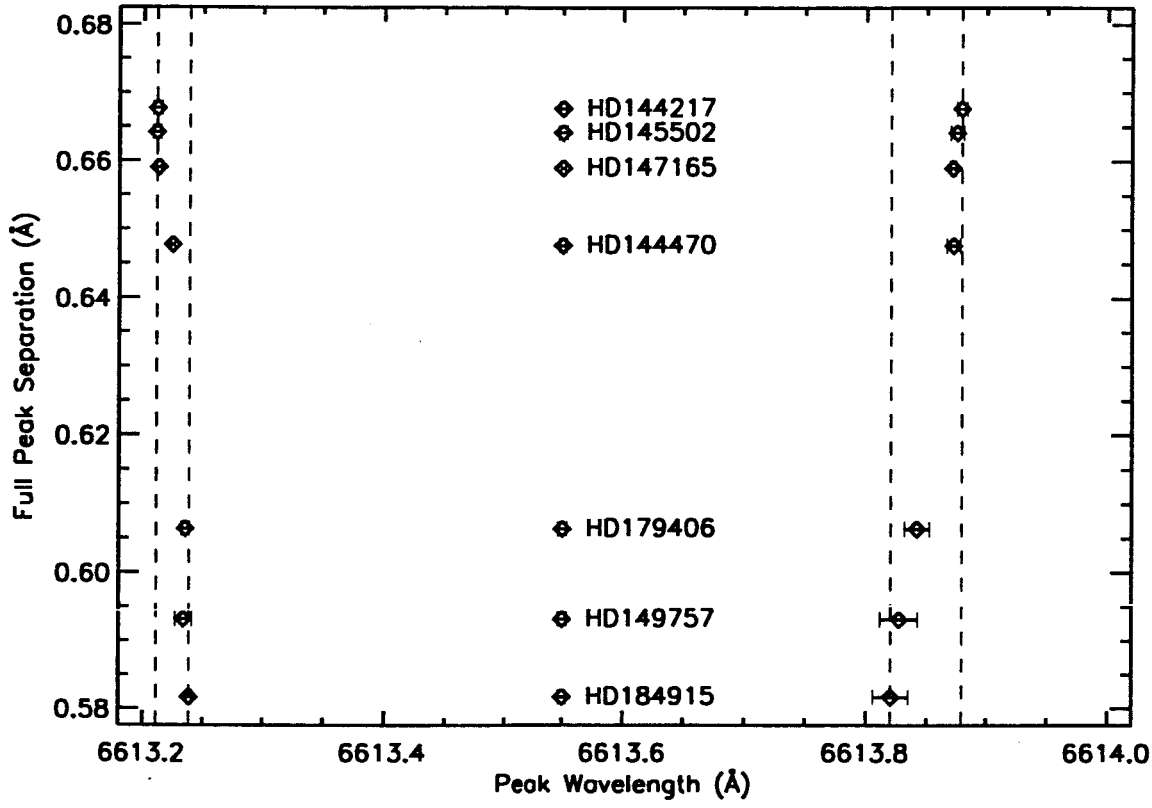

Fig. 2.— The peak positions for the three main peaks in the λ6614 DIB profile. Error bars are determined using a statistical approach (see text).

Table 1. The observed peak separations in the λ6614 DIB and derived $T_{\rm rot}$ and B'' values.

HD	$\Delta\nu_{12}$	$\Delta\nu_{23}$	$\Delta\nu_{13}$	$T_{\rm rot}$	$T_{\rm H_2}$[a]	B''
	Wavenumbers (cm^{-1})			K	K	10^{-3} cm^{-1}
HD 144217	0.774	0.753	1.527	$39\,^{133}_{23}$	88	$10.6\,^{21.3}_{0}$
HD 145502	0.775	0.743	1.518	$26\,^{64}_{16}$	90	$15.8\,^{29.0}_{2.7}$
HD 147165	0.771	0.735	1.507	$23\,^{30}_{18}$	64	$18.0\,^{24.3}_{11.6}$
HD 144470	0.744	0.736	1.481	$98\,^{102}_{32}$	73	$4.0\,^{14.8}_{0}$
HD 179406	0.719	0.667	1.386	$13\,^{29}_{8}$	–	$25.9\,^{43.8}_{8.0}$
HD 149757	0.723	0.633	1.356	$7\,^{14}_{5}$	54	$44.7\,^{71.7}_{17.6}$
HD 184915	0.712	0.618	1.330	$7\,^{11}_{5}$	69	$47.3\,^{68.4}_{26.1}$

[a]From Savage et al. (1977)